Вавиловский журнал генетики и селекции. 2023;27(3):250-263
DOI 10.18699/VJGB-23-31

LIM-kinase 1 effects on memory abilities and male courtship song in *Drosophila* depend on the neuronal type

A.V. Zhuravlev[1] ✉, E.S. Zalomaeva[1, 2], E.S. Egozova[2], A.D. Emelin[2], V.V. Sokurova[2], E.A. Nikitina[1, 2], E.V. Savvateeva-Popova[1]

[1] Pavlov Institute of Physiology of the Russian Academy of Sciences, St. Petersburg, Russia
[2] Herzen State Pedagogical University of Russia, St. Petersburg, Russia
✉ beneor@mail.ru

Abstract. The signal pathway of actin remodeling, including LIM-kinase 1 (LIMK1) and its substrate cofilin, regulates multiple processes in neurons of vertebrates and invertebrates. *Drosophila melanogaster* is widely used as a model object for studying mechanisms of memory formation, storage, retrieval and forgetting. Previously, active forgetting in *Drosophila* was investigated in the standard Pavlovian olfactory conditioning paradigm. The role of specific dopaminergic neurons (DAN) and components of the actin remodeling pathway in different forms of forgetting was shown. In our research, we investigated the role of LIMK1 in *Drosophila* memory and forgetting in the conditioned courtship suppression paradigm (CCSP). In the *Drosophila* brain, LIMK1 and p-cofilin levels appeared to be low in specific neuropil structures, including the mushroom body (MB) lobes and the central complex. At the same time, LIMK1 was observed in cell bodies, such as DAN clusters regulating memory formation in CCSP. We applied GAL4 × UAS binary system to induce *limk1* RNA interference in different types of neurons. The hybrid strain with *limk1* interference in MB lobes and glia showed an increase in 3-h short-term memory (STM), without significant effects on long-term memory. *limk1* interference in cholinergic neurons (CHN) impaired STM, while its interference in DAN and serotoninergic neurons (SRN) also dramatically impaired the flies' learning ability. By contrast, *limk1* interference in *fruitless* neurons (FRN) resulted in increased 15–60 min STM, indicating a possible LIMK1 role in active forgetting. Males with *limk1* interference in CHN and FRN also showed the opposite trends of courtship song parameters changes. Thus, LIMK1 effects on the *Drosophila* male memory and courtship song appeared to depend on the neuronal type or brain structure.
Key words: *Drosophila*; LIMK1; conditioned courtship suppression paradigm; memory; forgetting; dopaminergic neurons; cholinergic neurons; *fruitless*; male courtship song.

For citation: Zhuravlev A.V., Zalomaeva E.S., Egozova E.S., Emelin A.D., Sokurova V.V., Nikitina E.A., Savvateeva-Popova E.V. LIM-kinase 1 effects on memory abilities and male courtship song in *Drosophila* depend on the neuronal type. *Vavilovskii Zhurnal Genetiki i Selektsii = Vavilov Journal of Genetics and Breeding*. 2023;27(3):250-263. DOI 10.18699/VJGB-23-31

Влияние LIM-киназы 1 на память и брачную песню самцов дрозофилы зависит от типа нейронов

А.В. Журавлев[1] ✉, Е.С. Заломаева[1, 2], Е.С. Егозова[2], А.Д. Емелин[2], В.В. Сокурова[2], Е.А. Никитина[1, 2], Е.В. Савватеева-Попова[1]

[1] Институт физиологии им. И.П. Павлова Российской академии наук, Санкт-Петербург, Россия
[2] Российский государственный педагогический университет им. А.И. Герцена, Санкт-Петербург, Россия
✉ beneor@mail.ru

Аннотация. Сигнальный каскад ремоделирования актина, в состав которого входят LIM-киназа 1 (LIMK1) и ее субстрат кофилин, участвует в регуляции различных процессов в нейронах позвоночных и беспозвоночных животных. *Drosophila melanogaster* широко используется как модельный объект для изучения механизмов формирования, сохранения и воспроизведения памяти, а также забывания. Ранее активное забывание у дрозофилы исследовали с помощью классического павловского ольфакторного обучения. Было показано, что в разных формах забывания участвуют специфические дофаминергические нейроны и компоненты актинового каскада. В данной работе мы оценивали роль LIMK1 в процессах памяти и забывания у дрозофилы в парадигме условно-рефлекторного подавления ухаживания. В мозге дрозофилы уровень LIMK1 и фосфокофилина избирательно снижен в отдельных структурах нейропиля, включая лопасти грибовидных тел и центральный комплекс. В то же время LIMK1 присутствует в телах нервных клеток, таких как кластеры дофаминергических нейронов, регулирующие формирование памяти при условно-рефлекторном подавлении ухаживания. С использованием системы бинарного скрещивания GAL4 × UAS мы инициировали РНК-интерференцию *limk1* в различных типах нервных клеток. У гибридных линий с интерференцией *limk1* в лопастях грибовидных тел и глии наблюдалось усиление 3-часовой краткосрочной памяти, без видимого влияния на долгосрочную память. Интерференция *limk1* в холинергических нейронах приводила к снижению краткосрочной памяти, в дофаминергических и серотонинергических нейронах ее результатом было также существенное нарушение способности мух к обучению. Напротив, интерференция *limk1* в нейронах *fruitless* усиливала 15–60-минутную краткосрочную память, что указывает на возможную роль LIMK1 в процессах активного забывания. У самцов с интерференцией *limk1* в

холинергических и *fruitless* нейронах также были отмечены разнонаправленные изменения параметров брачной песни. Таким образом, эффекты LIMK1 на память и брачную песню самцов дрозофилы определяются типом нервных клеток или структурой мозга.
Ключевые слова: дрозофила; LIMK1; условно-рефлекторное подавление ухаживания; память; забывание; дофаминергические нейроны; холинергические нейроны; *fruitless*; брачная песня самца.

Introduction

Memory formation and forgetting serve as the basis of behavioral plasticity. Whereas memory is a specific process of information acquisition, storage and retrieval by the nervous system, active forgetting is defined as "a mechanism or series of mechanisms to remove memories that become unused" (Davis, Zhong, 2017). Associative memory formation and active forgetting occur in both mammals and invertebrates, including *Drosophila melanogaster* (Medina, 2018), which is a well-known object of classical genetics. Having a short life cycle and relatively simple nervous system, the fruit fly makes it easy to perform genetic analysis of the molecular basis of behavioral and cognitive processes.

There are several experimental techniques to form associative memory in *Drosophila*, including short-term memory (STM) and protein synthesis-dependent long-term memory (LTM). The most widely used technique is classical Pavlovian learning with negative electroshock reinforcement, or olfactory aversive learning (OAVL), which revealed genes responsible for different types of memory (Tully et al., 1994). More natural is conditioned courtship suppression paradigm (CCSP) (Siegel, Hall, 1979; Kamyshev et al., 1999). GAL4 × UAS binary expression system (Duffy, 2002) is used to study the effects of specific genes on memory processes. The fine neural organization of the mushroom bodies (MB), a principle structure responsible for associative olfactory learning in *Drosophila*, was evaluated in detail. The MB output neurons (MBON) are the main effectors of MB, whereas specific clusters of dopaminergic neurons (DAN) regulate the activity of MB – MBON synaptic contacts (Aso et al., 2009, 2014a, b). Among them are aSP13 DAN of the protocerebral anterior medial cluster (PAM), which innervate γ5 area of MB, playing a crucial role in CCSP learning and memory (Keleman et al., 2012).

The molecular and neural mechanisms of active forgetting implicate the activity of DAN and Rac1-dependent signal pathways (Medina, 2018). Small GTPases of the Rho family, including Rho and Rac, regulate neuronal actin polymerization during the *Drosophila* nervous system development. Rho *via* its effector ROCK or Rac/Cdc42 *via* its effector Pak activate LIM-kinase 1 (LIMK1), which phosphorylates *Drosophila* cofilin (twinstar) protein, blocking its actin-depolymerization activity and inhibiting axon growth. Rac also acts through Pak-independent pathway to antagonize LIMK1 and promote axon growth (Ng, Luo, 2004). In addition to its role in neurogenesis, Rac is crucial for both interference-induced and passive forgetting in OAVL paradigm. PAK/LIMK1/cofilin pathway probably acts downstream Rac1 (Shuai et al., 2010). Forgetting specific types of memory depends on different signal proteins (Zhang et al., 2016; Gao et al., 2019).

Forgetting in OAVL paradigm is caused by several DAN of the protocerebral posterior lateral 1 (PPL1) cluster, which innervates some MB structures, such as pedunculus, lower and upper stalk. Memory acquisition and forgetting are regulated by different dopamine receptors, dDA1 and DAMB respectively (Berry et al., 2012). Coincidence of conditioned and unconditioned stimuli creates a memory trace in MBON-γ2α′1, probably inhibiting the MB > MBON-γ2α′1 synapses. The unconditioned stimulus alone activates DAN-γ2α′1, which in turn disinhibit MB > MBON-γ2α′1 synapses and cause forgetting (Berry et al., 2018). DAN that innervate the MB αα′ tip induce the interference-based forgetting through the scaffold protein Scribble, binding together Rac1, PAK3 and cofilin (Cervantes-Sandoval et al., 2016).

Whereas multiple data prove the importance of DAN and actin-remodeling signal pathway for forgetting in OAVL paradigm, there is virtually no data for molecular mechanisms of memory decay in CCSP. Effects of LIMK1-dependent signal cascade on CCSP learning and memory were firstly shown for the temperature-sensitive mutant agn^{ts3}, with LIMK1 increase in the adult brain compared to the wild type *Canton-S* (*CS*). Temperature rise leads to a decrease in agn^{ts3} LIMK1 level, simultaneously restoring its learning ability and 3 h memory, which are drastically impaired in the norm (Medvedeva et al., 2008). agn^{ts3} has multiple polymorphisms within and near *limk1* gene, as well as a changed profile of microRNA expression, and can serve as a model object for Williams syndrome (Nikitina et al., 2014; Savvateeva-Popova et al., 2017). The temporal profile of STM learning index (LI) was assayed in CCSP for agn^{ts3}, as well as for the wild-type strains with *limk1* polymorphisms, *CS* and *Oregon R*. Only *CS* was able to learn and store memory up to 24 h (Zalomaeva et al., 2021).

The behavioral effects of LIMK1 changes in agn^{ts3} do not give information about specific cell types, where LIMK1 can be involved in learning and memory. In this study, we performed the analysis of memory decay for several *Drosophila* GAL4 × UAS strains with neuronal type-specific *limk1* RNA interference. LIMK1 distribution in the *Drosophila* brain structures was studied in detail using confocal microscopy. The effect of *limk1* interference on fly memory ability depended on both neural type and memory form. LIMK1 also appeared to be involved in regulation of male courtship song: *limk1* interference in different neuronal types specifically affected some song parameters.

Materials and methods

***Drosophila* strains.** Fly strains were provided by the Research Center "Biocollection of Pavlov Institute of Physiology RAS for the study of integrative mechanisms of the nervous and visceral systems". The strain numbers (#) are given in accordance with the Research Center and Bloomington *Drosophila* Stock Center, USA (Cook et al., 2010). The following strains were used:

1. *Canton-S* (*CS*) – the wild-type strain with *limk1* polymorphisms.
2. agn^{ts3} – temperature-sensitive mutation on *CS* genetic background with *limk1* polymorphisms, characterized by learning and memory defects.

3. Strains expressing GAL4 in specific neuronal types:
   #6794: w[*]; P{w[+mC]=nrv2-GAL4.S}8 P{w[+mC]=UAS-GFP.S65T}eg[T10]. GAL4 and green fluorescent protein (GFP) are expressed in nervous system under *Nrv2* regulatory element;
   #6793: w[*]; P{w[+mC]=ChAT-GAL4.7.4}19B P{w[+mC]=UAS-GFP.S65T}Myo31DF[T2]. GAL4 and GFP are expressed in cholinergic neurons (CHN) under *ChAT* and *VAChT* regulatory elements;
   #7009: w[1118]; P{w[+mC]=Ddc-GAL4.L}Lmpt[4.36]. GAL4 is expressed in dopaminergic (DAN) and serotoninergic (SRN) neurons;
   #30027: w[1118]; P{w[+mW.hs]=GawB}fru[NP0021]. GAL4 is expressed in *fruitless* neurons regulating mating behavior.
4. Act-GAL4: w[1118]; P{w[+mC]=} 25FO1/CyO, y[+]; *Canton-S* background. GAL4 is expressed in the whole body under actin promoter.
5. Strains with UAS-dependent *limk1* suppression:
   #26294: y[1] v[1]; P{y[+t7.7] v[+t1.8]=TRiP.JF02063}attP2. The strain expresses interfering RNA against *limk1* (RNAi) under UAS (*limk1-KD*, knockdown).
   #36303: y[1] v[1]; P{y[+t7.7]=CaryP}attP2. The control strain with genetic background identic to that for #26294, but lacking RNAi (*limk1*"+").
6. Strains with GFP gene regulated by UAS:
   #32186: w[*]; P{y[+t7.7] w[+mC]=10XUAS-IVS-mCD8::GFP}attP40.
   #32202: w[*]; P{y[+t7.7] w[+mC]=10XUAS-IVS-GFP-WPRE}attP2.

To induce *limk1* RNA interference in specific neuronal types, a strain carrying GAL4 activator expressed under tissue-specific promoter was crossed to UAS strain #26294. The cross product of a GAL4 strain and #36303 strain served as a control.

Flies were raised on the standard yeast–raisin medium at 25±0.5 °C and a 12:12 daily illumination cycle. For behavioral tests, experimental males were collected without anesthesia and kept individually. 5–6-day-old males were used in experiments. Females (*CS*) were collected as virgins and brought together with *CS* males for fertilization in CCSP one day before experiment.

Antibodies. Primary antibodies: Rat anti-LIMK1 multispecific monoclonal (Enzo Life Sciences, ALX-803-343-C100); mouse anti-*Drosophila* cysteine string protein (CSP); rabbit anti-*Drosophila* tyrosine hydroxylase (TH) (Abcam, ab128249); rabbit anti-GFP (Abcam, ab290).

Secondary antibodies: Goat anti-mouse Alexa Fluor 488 (Invitrogen, A32723), donkey-anti-rat Alexa Fluor 594 (ThermoFisherScientific, A-21209), goat anti-rabbit Alexa Fluor 633 (Invitrogen, A21071).

RNA extraction and RT-PCR analysis of *limk1* expression. The level of *limk1* expression was assayed using semi-quantitative PCR in complex with reverse transcription (RT-PCR). Flies were anesthetized by freezing. 10 male flies or 70 male heads were homogenized in 300 µl TRI reagent (MRC, TR 118). Total RNA was extracted from homogenates according to the manufacturer's protocol. The quality of RNA was checked by 1.5 % agarose gel electrophoresis. 1 µg RNA was reverse-transcribed by MMLV reverse transcriptase (Evrogen, #SK022S) according to the manufacturers' protocol, using random hexamer primers and RNAse inhibitor (Syntol, #E-055). Semi-quantitative PCR was performed on a StepOne Plus (Applied Biosystems, Inc., USA) using qPCRmix HS SYBR+LowROX (Evrogen, # PK156L) containing direct and reverse primers (0.5 mM each). Baseline and cycle threshold values were determined by automatic analysis using StepOne software v2.3 (Applied Biosystems, USA). *rpl32* transcript was used as an internal control. The predesigned *limk1* primers (PP12636 in FlyPrimerBank, http://www.flyrnai.org/flyprimerbank) were used to bind all five *limk1* cDNA isoforms, both premature and mature forms, as primers do not span the exon-intron borders. The relative *limk1* transcript level was calculated using the comparative ΔΔCt method. The number of biological replicates (independent RNA extractions with reverse transcription) was 3–5, the number of technical replicates was 3.

The primer sequences were the following:
rpl32:
Forward: 5′-TATGCTAAGCTGTCGCACAAATGGC-3′
Reverse: 5′-GTTCTGCATGAGCAGGACCTCCA-3′
limk1:
Forward: 5′-GTGAACGGCACACCAGTTAGT-3′
Reverse: 5′-ACTTGCACCGGATCATGCTC-3′
PCR parameters:

1. 1 cycle: 95 °C – 5 min.
2. 45 cycles. 95 °C – 20 s, 60 °C – 20 s, 72 °C – 20 s, 77 °C – 15 s (detection).
3. Melting curve: 95 °C – 15 s, 60 °C – 1 min, 60–95 °C (Δ 0.3 °C, 15 s).

Immunofluorescent staining of *Drosophila* brains. 5–6-day-old imago males were anesthetized by freezing. The brains were prepared in PBS buffer (pH 7.5) using needle-sharp tweezers (Merck, T4412), fixed in 4 % paraformaldehyde in PBS for 1 h at RT and stained according to (Thapa et al., 2019), without a freezing stage. Antibodies were diluted in PBT (0.2 % Tween 20, 5 % BSA in PBS) as 1:200, for anti-CSP – 1:20. Previously, for better staining of brains, we increased the time of incubation with primary antibodies up to 5 days (Zhuravlev et al., 2020). Here, the incubation was performed at 4 °C for 3 days (with primary antibodies) or overnight (with secondary antibodies). Brains were mounted with Vectashield mounting medium containing DAPI (Vector laboratories, H-1200-10).

Protein distribution analysis in the brain by confocal microscopy. Brains were scanned frontally using laser scanning confocal microscopy (LSM 710 Carl Zeiss; Confocal microscopy Resource Center; Pavlov Institute of Physiology of the Russian Academy of Sciences, St. Petersburg, Russia). Scanning was performed using X63 objective at different depths (z-step 2 µm). Images were analyzed using Fiji software. The brain structures were visually mapped using the *Drosophila* brain online atlas (Virtual Fly Brain). To measure the average level of LIMK1 inside the brain structures, the average signal intensity was measured in three small square areas (~10 × 10 µm) within each of the structures. The average values were obtained and normalized to the average structure intensity for the given brain. Colocalization Threshold analysis

was performed to measure co-localization of LIMK1 with neurospecific markers. To prepare figures, auto contrast function was used for each optical slice.

Learning and courtship suppression tests in *Drosophila* males. Flies learning and STM were estimated in CCSP, as described in (Zhuravlev et al., 2022). In the case of long term memory (LTM), learning was performed by placing flies in food-containing glasses (20 mm diam., ~20 mm high) for 5 h (Kamyshev et al., 1999). Courtship index (CI) and learning index (LI) were estimated at the following time points after learning: for short-term memory (STM) analysis: 0 min (learning), 3 h; for STM decay analysis: 15, 30, 60 min, 24 h; for LTM analysis: 0 min, 2 days, 8 days. In all groups, naive males (without mating experience) served as a control to calculate LI:

$$LI = [(CI_N - CI_T)/CI_T] \times 100\ \% = (1 - CI_N/CI_T) \times 100\ \%,$$

where CI_N is the middle CI for naive males, and CI_T is the middle CI for males after training. The naive and trained males were the same age. The decrease in LI compared to LI (0 min) was considered a time-dependent memory decay. The decrease in LI for a mutant strain compared to that for the wild-type strain *CS* was considered a strain-specific impairment of learning or memory.

Courtship song analysis. The 5-day-old imago male courtship song was recorded as in (Savvateeva-Popova et al., 2008). A naive male of the studied line and a fertilized female (*CS*) were placed together in a Perplex chamber with a latticed bottom on top of a microphone. The chamber was placed in a foam box in a soundproof room. The sounds were recorded for 5 min using Audacity software (Mazzoni, Dannenberg, 2020). The sound signals were filtered to exclude noises, obtaining signals within 100–800 Hz. The level of noise was decreased using a standard Audacity plugin. The software *Drosophila* courtship song analysis (DCSA) (Iliadi et al., 2009) was used to automatically detect pulse and sine song components.

The results of analysis were manually edited. The mean values of the song parameters were calculated for each fly. The following parameters were estimated: pulse song index (PInd, % of the total time), pulse song initiation frequency (PFr; 100/s), sine song index (SInd, % of the total time), sine song frequency (SFr, 100/s), interpulse interval (IPI, ms), period of song pulse train (Per, s), intertrain interval (ITI, ms), train duration (TrainDur), pulse number in train (PulseN), sine song duration (SDur, ms), sine song amplitude (SAmp, C.U.), IPI variance (Var(IPI), ms^2). Per is the time between the starts of the neighboring trains. ITI is the time between the end of the previous and the start of the next train.

Statistical analysis. Analysis of LIMK1 mRNA level was performed using two-sided *t*-test, Social Science Statistic online resource ($p < 0.05$). Analysis of LI and courtship song parameters was performed using two-sided randomization test at significance level α of 0.05 ($n = 20$), using *Drosophila* Courtship Lite software (Nikolai Kamyshev, 2006, nkamster@gmail.com), with 10000 iterations. The program is freely available from the author upon request. Randomization test was reported to be better for LI comparison than *t*-test or some nonparametric tests (Kamyshev et al., 1999). Courtship song parameters were also analyzed using two-sided Mann–Whitney U-test. Python 3 scripts were used to draw the box plots charts.

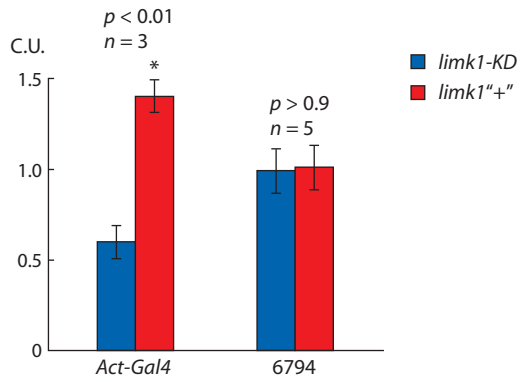

Fig. 1. Comparative levels of *limk1* RNA in the UAS > GAL4 hybrids with and without *limk1* RNA interference.

X axis: GAL4 strains. *Y* axis, conditional units (C.U., expression levels are normalized to the average value). Statistical differences: * between *limk1-KD* > GAL4 and *limk1"+"* > GAL4 (two-sided *t*-test; *p* and *n* are shown above the charts). Standard error is shown.

Results

limk1 RNA level in Drosophila UAS × GAL4 hybrids

To check that GAL4 really induces *limk1* RNA interference in 26294 strain, we compared *limk1* RNA level in the UAS (f) > GAL4 (m) hybrids. Females with and without transgenic RNAi for *limk1* suppression (*limk1-KD* and *limk1*"+", respectively) were crossed to *Act-GAL4* males, expressing GAL4 in the whole body. The level of total *limk1* RNA was approximately 2-fold lower in the hybrid with *limk1* interference. These data confirmed the efficiency of RNAi-dependent *limk1* suppression in 26294 strain (*limk1-KD*) upon its activation by GAL4. At the same time, there were no differences for *limk1-KD* > 6794 and *limk1*"+" > 6794, where RNA expression was measured in heads and was regulated by neuronal type-specific GAL4 (Fig. 1). Thus, *limk1* RNA differences after neural type-specific *limk1* RNA interference might be local or too low to be detected in the whole *Drosophila* heads.

LIMK1 distribution in the *Drosophila* brain

When studying LIMK1 distribution, we focused on the central part of the *Drosophila* brain, without the optic lobes (OL), mainly at the level of the superior medial protocerebrum (SMP) and gamma-lobes (γL) of MB. Here the PAM clusters of DAN are located (Mao, Davis, 2009), responsible for the *Drosophila* courtship learning and memory (Keleman et al., 2012). Additionally, the area including the central complex (CC) and calyx (Cal) surrounded by Kenyon cells (KC) was studied. The CSP-positive neuropil structures and tyrosine hydroxylase (TH)-positive DAN cell bodies and processes served as landmarks in describing the LIMK1 distribution. The following description is given for the wild-type strain *CS* (see the Table and Suppl. Material 1)[1].

[1] Supplementary Materials 1–6 are available in the online version of the paper: https://vavilovj-icg.ru/download/pict-2023-27/appx9.pdf

LIMK1 and TH distribution in the *Canton-S* brain (visual analysis)

Z	N	Neuropil structures (CSP)	TH-positive structures	LIMK1 level
I	0	AL and SMP; the part of γL is observed as a shading (CSP lever is lower)	Two bilaterally symmetrical clusters of PAM cell bodies, the processes of which form two semicircular tracts (#1), enveloping SMP below	AL and SMP: high; thin tissue layers resembling the neuropil glia: high; cell bodies surrounding neuropil: relatively low; cell nuclei: low
II	3	γL of MB, subdivided into three unequal parts; the putative γ5 area is marked with an asterisk (*); AOT lateral to SMP	Semicircular tracts (#1) move laterally; two tracts (#2) above SMP; granularity (#3) above γL. TH level is low in γL	γL: lower than in SMP; the thin tissue layers surrounding AL and SMP: high
III	7	γL is half hidden by β′L, with the horizontal βL below it. The beginning of α/α′L is seen	Granularity (#3) above and laterally the β′L area; tracts (#2) join at the central line (#4). TH level is low in βL	All MB lobes: low
IV	11	αL and α′L. The part of γL (#7) lateral to αL	Granularity (#5) at the area of β′L tips, where the PAM processes converge	Area #5: low; granularity along the central axis of the brain (#6): high; γL (#7): very low
V	14	The tips of αL and α′L; the part of EB	Area 5 is subdivided into two (#8), corresponding to β′L tips. Commissure (#9) above (#8)	Area #8: low; EB: low
VI	16	EB; αL and γL join to the pedunculus (Ped) of MB	Commissure #9 above EB	Ped and EB: low; the semicircular granularity (#10) above and laterally EB: high; commissure (#11) between EB and the esophagus (ES): high
VII	20	CC (EB, FB and No)	Commissure #9 continues laterally	CC and Ped: low; tissue layers surrounding neuropil structures: high
VIII	26	CC (FB), W, Ped	Tracts around FB	Commissure (#12) above CC and semicircular structures (#13) surrounding wedge: high
IX	29	CC is no longer visible	The cell bodies and processes of DAN clusters around Cal are partly visible	The great commissure (#GC) above the ES: high; glia-like layers among neuropil: high
X	36	Cal, KC and PB; Ped below Cal – a small shading (#14)	DAN clusters around Cal: PPL1 and PPM2	Cal and PB: high; KC: relatively low; glia-like layers (#15) in the bottom part near ES: high

Note. The depth of the studied zone (Z) is given for the brain optical slices, from the PAM cell bodies to CC (I–V) or from CC to Cal (VI–X). N is the number of the brain optic slice for a given zone (step 2 μm). For different brains, there may be slight differences in depth of the given N.
The brain structures (here and below): α, α′, β, β′ and γL – the corresponding lobes of MB, AL – the antennal lobes, AOT – the anterior optic tubercule, Cal – the calyx of MB, CC – the central complex, EB – the ellipsoid body of CC, ES – the esophagus, FB – the fan-shaped body of CC, KC – the Kenyon cells, MB – the mushroom body, MBl – the median bundle, No – the noduli of CC, PB – the protocerebral bridge, Ped – the pedunculus of MB, SEG – the subesophageal ganglion, SMP – the superior medial protocerebrum, W – wedge. DAN clusters, according to (Mao, Davis, 2009): PAM – the protocerebral anterior medial cluster, PPL – the protocerebral posterior lateral clusters, PPM – the protocerebral posterior medial clusters.

The distribution of DAN clusters corresponded to that described in (Mao, Davis, 2009). PAM clusters were clearly observed near SMP, with processes extending towards the central part of the brain. The processes formed glomerular structures around the MB horizontal lobes (γ, β and β′L), probably being the synaptic endings innervating the correspond areas. The structure #3 was located above γL, the structures #5 and 8 – in the β′L area, the commissure #9 was seen in the central part of the brain. TH signal was relatively low in βL (see Suppl. Material 1). PPL1, PPM2 and other DAN clusters were observed around Cal, sending their processes to the different brain areas (Fig. 2, *a*).

LIMK1 was concentrated in the neuropil structures of the anterior part of the brain, such as SMP and AL. The LIMK1-positive granularity was observed inside SMP, between the β′L tips (#8) and around the ellipsoid body (EB) of CC (#10, 11). LIMK1 level was also high in thin tissue layers adjacent to neuropil and some neural tracts, such as #12 around the great commissure, #13 around wedge (W) and #15 near esophagus (ES), morphologically resembling glia (Hartenstein, 2011). LIMK1 signal was lower in cell bodies of the neurons surrounding AL (ALCB), probably being the cell bodies of the projection neurons, as well as in KC surrounding Cal. Here, LIMK1 was mainly concentrated in the cytoplasm, beyond the nuclei. LIMK1 level was significantly decreased in all the MB lobes and pedunculus (Ped), as well as in the CC structures, whereas in Cal and the protocerebral bridge (PB) it was relatively high (see Suppl. Material 1). LIMK1 and TH co-localization was observed in SMP, AL, Cal, the TH-positive cells and processes, and in glomerular densities, such as #3, 5 and 6 (see Fig. 2, *b*).

To check that the antibody specifically binds to LIMK1, the distribution of LIMK1 main product p-cofilin was assayed in *CS*. The pattern of p-cofilin distribution was generally similar to that for LIMK1 (Suppl. Material 2). The level of p-cofilin was low in MB (including Cal) and CC (mostly EB, as well as in the case of LIMK1). In contrast to LIMK1, p-cofilin was mainly concentrated in the cell nuclei in the peripheral area of the fly brain, such as Kenyon cells around Cal, as well as in PB, subesophageal ganglion (SEG), and cell bodies surrounding

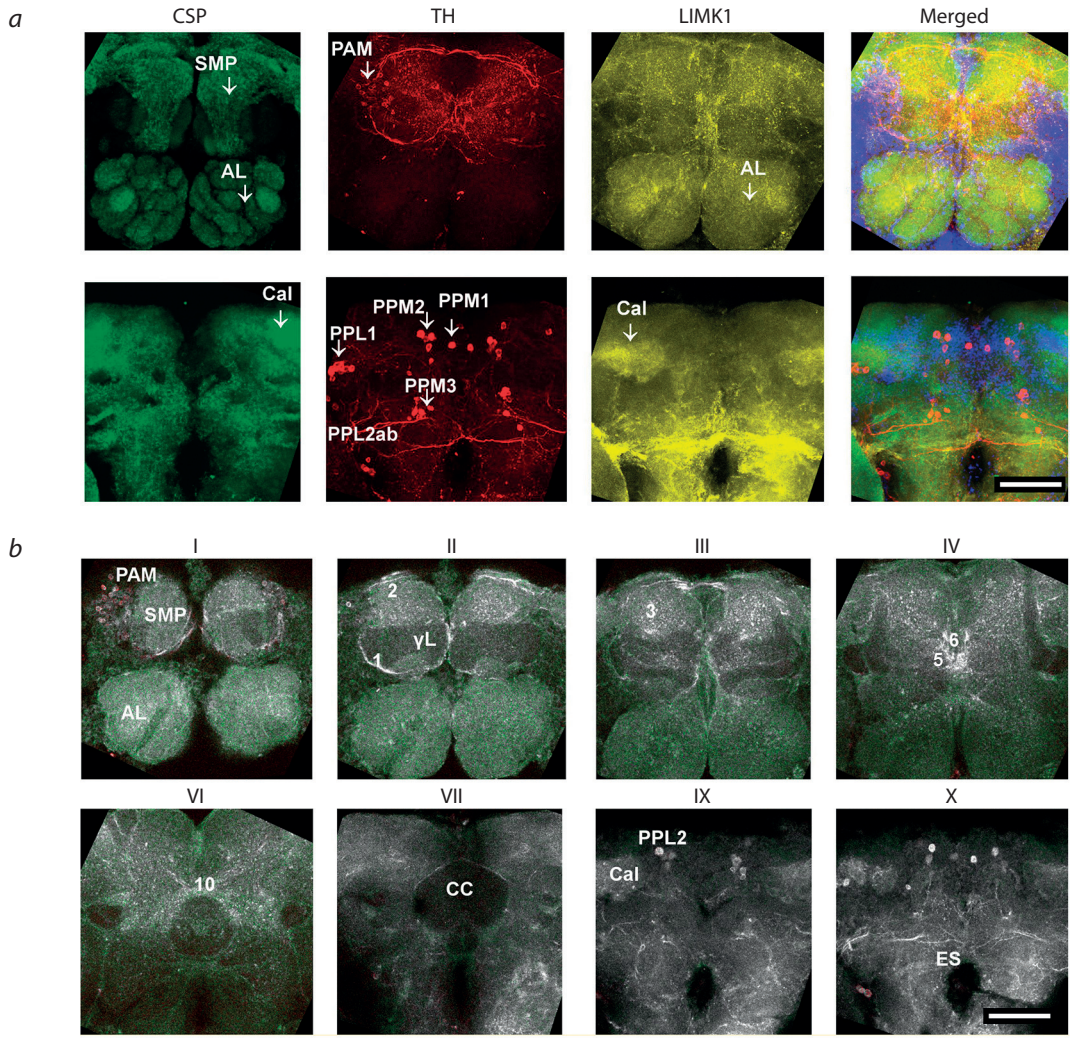

Fig. 2. LIMK1 spatial distribution in the *CS* brain.

a, Z-projection. AL level (above) and Cal level (below). Color scheme: green – CSP, red – TH, yellow – LIMK1, blue – DAPI. *b*, Co-localization of TH and LIMK1 in different optic zones. Color scheme: green – LIMK1, red – TH, white – the areas of LIMK1 – TH co-localization. The scale bar size is 50 μm. See the Table for abbreviations and description of the optic zones.

AL. p-Cofilin was also localized in diffuse layers within the brain structures, such as EB, probably formed by glia. The p-cofilin-enriched cells were found in SEG, forming structures with two glomerular branches (*), and around CC structures, fan-shaped body (FB) and EB (**).

Several GAL4 activators were used to initiate *limk1* RNA interference. Both 6793 and 6794 strains specifically express the green fluorescent protein (GFP) under GAL4 promoter. In strain 6794, GAL4 was reported to be expressed in OL, thoracic ganglion, different nerves, and cortex glia (Sun et al., 1999; Okamoto, Nishimura, 2015). In 6794 > *limk1-KD* hybrid, GAL4-driven GFP expression was detected in glia-like cells, surrounding the neuropil structures, such as AL, SMP, CC and its parts, as well as in the MB lobes, Ped and some KC (Suppl. Material 3, *a*). GFP level was higher in αL and βL compared to α′L, β′L and γL. The signal was lower in Cal and virtually absent in most neuropil structures, such as AL, SMP, CC and others. Thus, *limk1* interference should occur in Cal and some glia cells, where the levels of both GAL4 and LIMK1 were relatively high. Similar distribution was observed in the control 6794 > *limk1*"+" strain (see Suppl. Material 3, *b*). In the strain 6793, GAL4 is expressed in cholinergic neurons (CHN), with GFP signal in OL, AL with the surrounding interneurons, the parts of CC, the great commissure (GC), Cal and the mechanosensory area of SEG (Salvaterra, Kitamoto, 2001). In the strains 6793 > *limk1-KD* and 6793 > *limk1*"+" (see Suppl. Material 3, *c*, *d*), we observed a strong GFP signal in cell bodies surrounding SMP and AL, as well as in some KC, several neuropil structures (AL, α/βL, EB, FB), and GC. In all the studied strains, LIMK1 distribution character appeared to be similar to that in *CS*.

To check that GAL4 is active in 7009 and 30027 strains, we crossed them to strains expressing GFP under GAL4 promoter. In 7009 > 32186 hybrid, we observed a prominent GFP signal in cell clusters near SMP, morphologically similar to the TH-positive PAM clusters. Some cells might be SRN, but they constitute the minority of the observed neurons in this area (Albin et al., 2015; Kasture et al., 2018). The processes of PAM neurons extended to the horizontal MB lobes, including γL, and the densely innervated β′L tip (#5) connected by

a commissure, and to a much lesser extent the βL tip (Suppl. Material 4, *a*). EB was surrounded by the GFP-positive processes extending from different parts of the brain. The GFP-positive DAN around Cal were also observed. Hence, GAL4 activator of 7009 should suppress *limk1* inside DAN, including PAM neurons, which regulate memory storage in CCSP. The *fruitless*-positive neurons (FRN) are responsible for mating behavior. In 30027 > 32202 hybrid, we observed GFP in some KC, in the cell bodies located near SMP and AL, and glomerular structure, forming a ring-like structure around Ped (see Suppl. Material 4, *b*). Similar structures were described in (Yu et al., 2010). The distribution of LIMK1 in the hybrid strains with and without *limk1* knockdown in the above neurons was similar to that in *CS* (Suppl. Material 5).

The normalized intensity of LIMK1 signal was calculated for several brain structures (Fig. 3). The LIMK1 relative levels in specific structures were very similar for the *CS* brain and the average brain of all the strains. The biggest differences were observed for the TH-positive glomerular structure #6 (TH+(6)), which is possibly responsible for memory formation in CCSP. In the average brain, ALCB had the normalized LIMK1 level about 1. Compared to them, AL, SMP and TH+(6) structures had the higher LIMK1 level, whereas the MB lobes, EB and Ped had the lower LIMK1 level. In agn^{ts3}, AL and ALCB had the higher LIMK1 level compared to *CS*, whereas most of the rest studies structures had lower LIMK1 level. This corresponds to more contrast LIMK1 staining in agn^{ts3} relative to *CS* (Suppl. Material 6). There were no prominent differences after *limk1* knockout, except for several structures with minor changes. The interstrain differences might be local or beyond the resolution of the method.

3 h STM differs in hybrids with and without *limk1* interference

3 h STM was estimated for *limk1-KD* (f) > 6794 (m) and the control *limk1*"+" (f) > 6794 (m) hybrids. In both cases, we observed the decrease of courtship index (CI) after learning, with its partial recovery after 3 h. The box plot height was minimal for *CS* and rather big for UAS × GAL4 hybrids, showing that the value of courtship suppression significantly varied for individual flies. All strains were capable to learn in CCSP, with learning index LI (0 h) immediately after training of about 60–70 % (Fig. 4, *a*). The *CS* LI was still high after 3 h, indicating STM preservation, in agreement with (Zhuravlev et al., 2022). The strain with *limk1* interference also preserved STM: although its LI (3 h) was only about 20 %, it did not statistically differ from that for *CS*, as well as from LI (0 h). In the control strain, LI (3 h) decreased compared to LI (0 h) and did not differ from zero, indicating the impaired STM. Thus, while 3 h memory storage or retrieval was impaired in the control strain, *limk1* interference seems to improve 3 h STM. At the same time, it did not affect the impaired 8 day LTM, with only minor positive effect on 2 day LTM (see Fig. 4, *b*).

Neuron type-specific *limk1* interference differentially affects STM dynamics

To investigate the dynamics of STM decay in different strains with *limk1* interference, we performed LI analysis immediately and 24 h after learning (Fig. 5). To exclude the possible effect of eye color on learning and memory abilities, we applied GAL4 (f) > UAS (m) crossing scheme, where both the strain with *limk1* knockdown and the control strain had the same wild-type eye color. For 6794 activator (MB and glia), the control strain showed nearly the same LI within 24 h, whereas the strain with *limk1* interference demonstrated a steeper forgetting curve. Hence, 6794 > *limk1-KD* showed high LI after learning, but seemed to increase the speed of memory forgetting on the interval 0–30 min. *limk1* knockdown in CHN (6793) was associated with significant decrease of LI within 60 min after training.

For DAN and SRN activator (7009), both the strain with *limk1* interference and the control strain showed nearly the same dynamics of STM decay, except for 30–60 min period. *limk1* interference was associated with a dramatic defect on learning: LI did not differ from zero. LI (24 h) was negative in both hybrids, possibly being the effect of sensitization: males did not suppress the courtship activity but courted more actively some time after training. For FRN activator (30027), the effect of *limk1* knockdown was the opposite to that of MB/glia and CHN activators: *limk1* interference decreased the speed of forgetting, and LI (30 min) did not differ from zero. Thus, the effect of *limk1* interference on STM dynamics appeared to depend on the neuronal type.

LIMK1 interference in CHN and FRN neurons differentially affects courtship song parameters

Finally, we studied the influence of *limk1* interference on the male courtship song parameters. The hybrids with CHN and FRN drivers were studied (Fig. 6). There were no interstrain differences in interpulse interval (IPI), the species- and population-specific parameter (Ritchie et al., 1994), and IPI variance (Var(IPI)), the marker of neurodegenerative processes (Savvateeva-Popova et al., 2003). *limk1* interference in CHN (6793) decreased the pulse song index and frequency (PInd, PFr), increasing the mean period (Per), intertrain interval (ITI), train duration (TrainDur), sine song duration (Sdur) and train pulse number (PulseN). On the contrary, in the strain with FRN activator (30027), *limk1* interference resulted in PFr increase, as well as Per, ITI, SInd and SDur decrease. *limk1* knockdown by two different activators had the opposite effects on PInd, PFr, Per, ITI and SDur, leveling the initial differences between SInd, TrainDur and PulseN. Thus, *limk1* interference in CHN seemed to decrease the rate of switching from the singing mode to silence mode and back, resulting in longer trains and ITI, while *limk1* interference in FRN neurons generally had the opposite effect.

Discussion

In mammals, LIMK1- and cofilin-dependent actin remodeling is widely involved in regulation of synaptic processes, such as exocytosis, receptor trafficking and remodeling of dendritic spines. These processes underlay long-term potentiation (LTP), long-term depression (LTD) and different forms of memory. LIMK1 also affects gene expression through CREB and LTM formation. Deregulation of LIMK1-dependent actin remodeling is involved in multiple pathologies, such as Alzheimer's and Parkinson's diseases, Williams syndrome, schizophrenia, and autism (Ben Zablah et al., 2021).

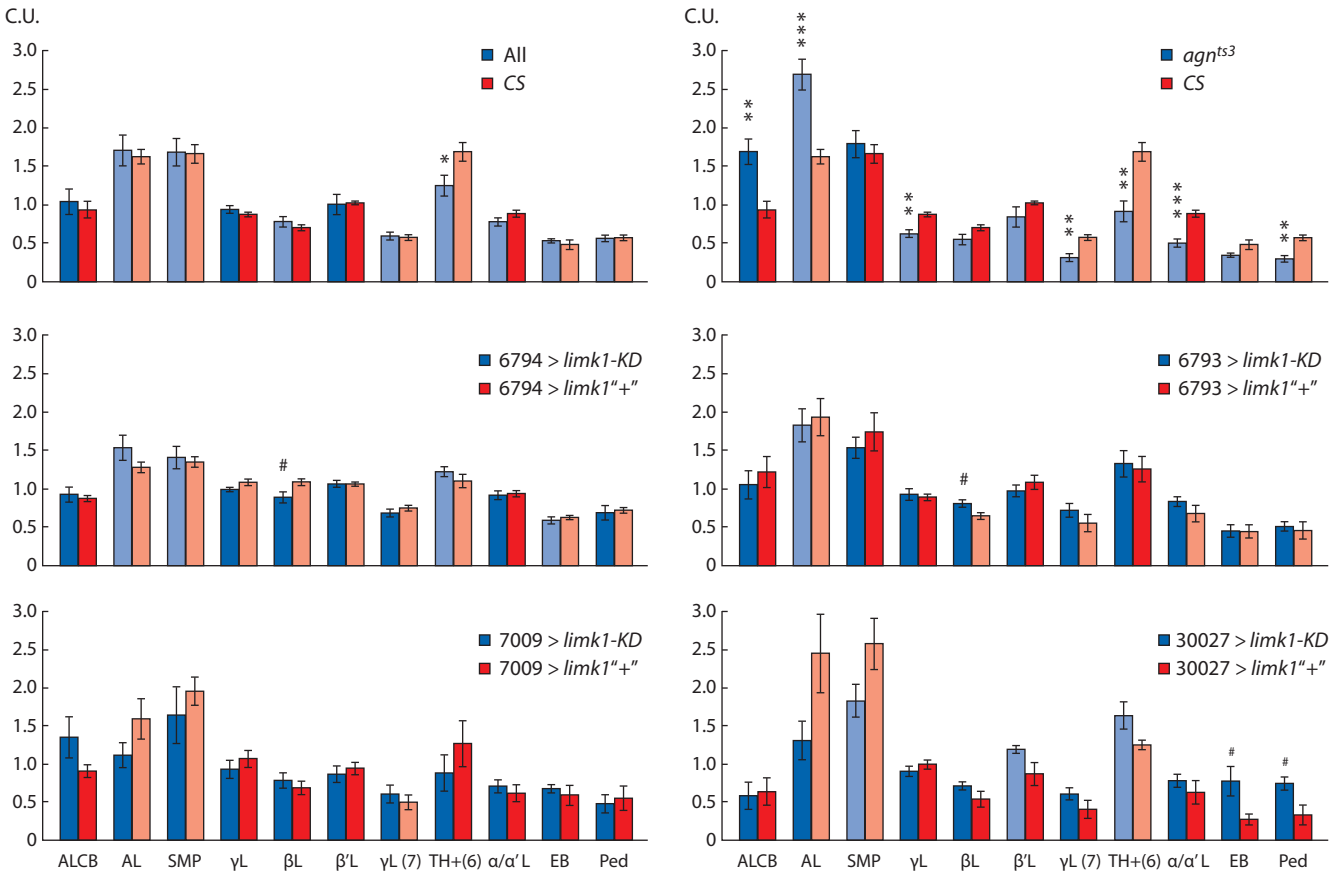

Fig. 3. LIMK1 relative level in different brain structures.

The normalized levels are shown in conventional units (C.U.). All – the averaged brain of the all studied strains. Statistical differences (two-sided *t*-test): * from *CS* ($p < 0.05$, 0.01, 0.001 for one, two and three asterisks, respectively); # from the control hybrid without *limk1* interference; blue > cyan and red > pink color change – the difference from ALCB ($p < 0.05$; blue and red – no difference). N = 47–61 (All), 5–6 (*CS*), 4–6 (*agn*^{ts3}), 7–8 (6794 > *limk1-KD*), 7–10 (6794 > *limk1*"+"), 5–6 (6793 > *limk1-KD*), 6–7 (6793 > *limk1*"+"), 3–5 (7009 > *limk1-KD*), 3–5 (7009 > *limk1*"+"), 4 (30027 > *limk1-KD*), 3–4 (30027 > *limk1*"+"). Standard error is shown.

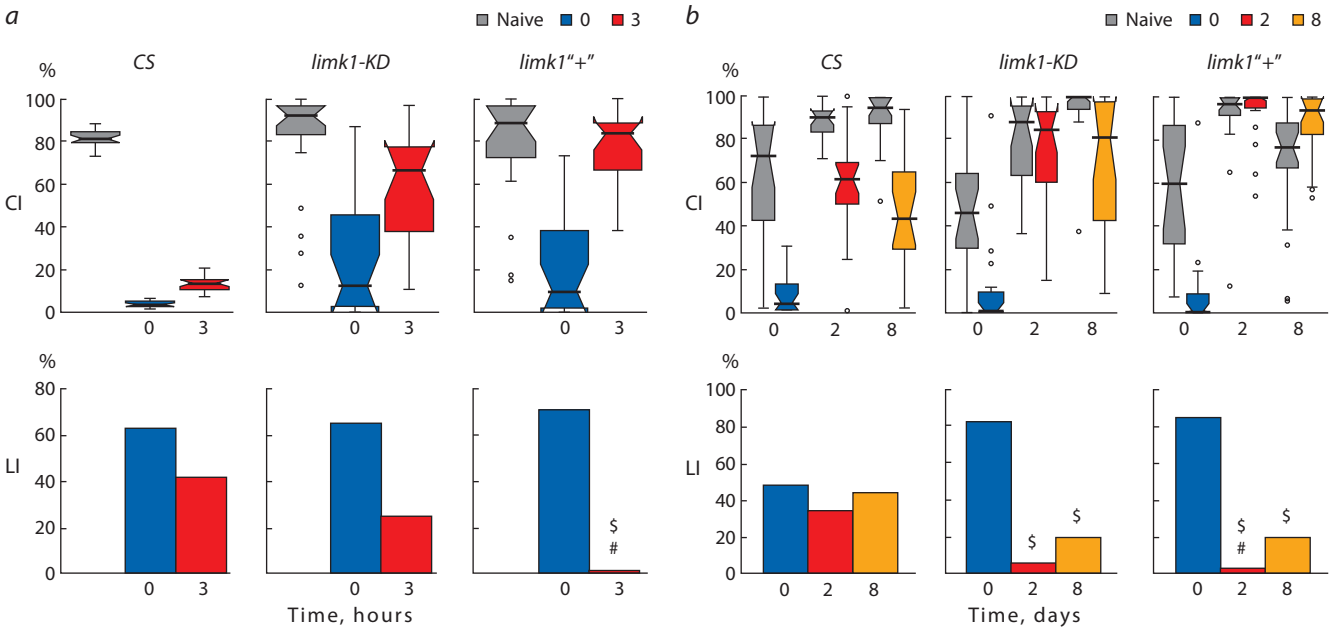

Fig. 4. The memory abilities of the *Drosophila* strain with *limk1* suppression by 6794 activator.

a, STM. *b*, LTM. CI – courtship index; box plot and whisker chart, median is shown by the bold black line. LI – learning index. Statistical differences: # from *CS*, $ from LI (0 h/0 day) (two-sided randomization test; $p < 0.05$, $n = 20$).

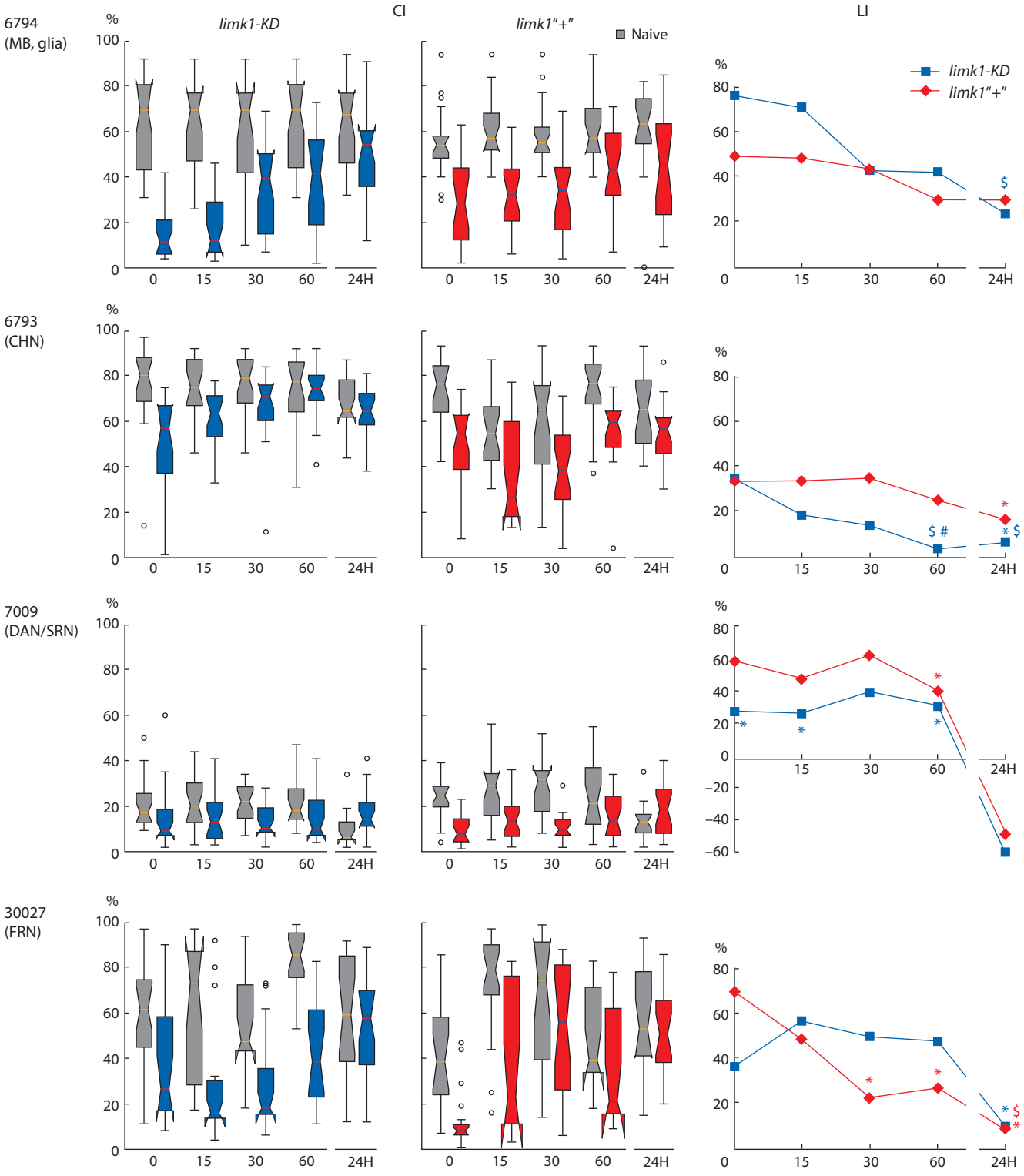

Fig. 5. STM dynamics in *Drosophila* strains with neuron type-specific *limk1* suppression.

CI – courtship index, LI – learning index. *X* axis: time (min; 24H – 24 hours). Statistical differences: # from *CS*, $ from LI (0 min), * no difference from zero (two-sided randomization test; $p < 0.05$, $n = 20$).

In mature neurons, actin is enriched in both pre- and postsynaptic structures, such as dendritic spines, regulated by Rho signaling pathway. The action of LIMK1 on actin polymerization and memory processes is rather complex, being dependent on the mode of LIMK1 regulation (transient or long-term overexpression) and cofilin level. While the active cofilin destabilizes fibrillar actin, in high concentrations it increases actin polymerization and nucleates actin filaments in dendritic spines during long-term potentiation (reviewed in Cuberos et al., 2015). Thus, it is hard to predict the integral

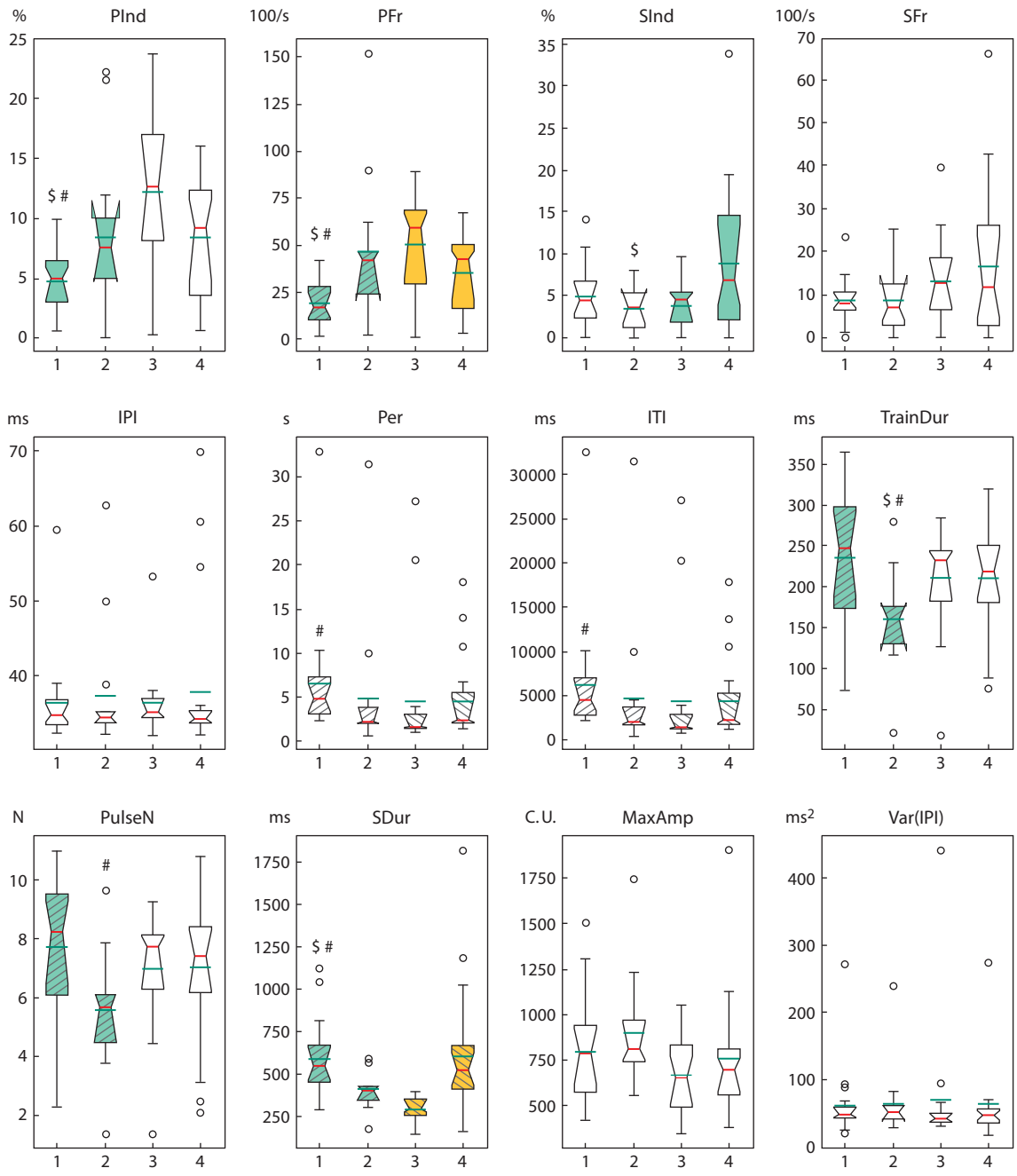

Fig. 6. Courtship song parameters in *Drosophila* hybrids with neuron type-specific *limk1* interference.

Hybrid numbers: 1. 6793 > *limk1-KD*; 2. 6793 > *limk1*"+" (CHN); 3. 30027 > *limk1-KD*; 4. 30027 > *limk1*"+" (FRN). Statistical differences: hybrids with *limk1* interference *vs* control – the pairs with difference are shown by color (two-sided randomization test, $p < 0.05$) or hatching (two-sided Mann–Whitney test, $p < 0.05$); hybrids with CHN driver *vs* hybrids with FRN driver: $ two-sided randomization test; # two-sided Mann–Whitney test. For hybrids 1, 2, 3, 4, respectively: $n = 20, 15, 17, 22$ for pulse song parameters; $n = 18, 13, 15, 20$ for sine song parameters. Median is shown by the red line, the mean value is shown by the green line.

effect of LIMK1 and cofilin activity on memory processes. It was crucial to check the behavioral effects of *Drosophila limk1* suppression in specific types of neurons.

Using paraffin section staining, both LIMK1 and its product p-cofilin were shown to be homogeneously distributed in the brain neuropil, with maximum level in CC (Lopatina et al., 2007). Our results of the confocal microscopy analysis gave a different picture of LIMK1 distribution, quite similar for all the studied strains. We have shown a specific LIMK1 decrease in MB, which is responsible for associative learning, as well as in CC, involved in higher movement control (Strauss, Heisenberg, 1993). This puts under question the role of LIMK1 in the aforementioned processes. However, LIMK1 was present in the cell bodies and processes of DAN, which interact with MB and CC (Mao, Davis, 2009) and regulate memory and forgetting. The observed p-cofilin distribution resembled this for LIMK1: its level was low in the MB lobes and CC. The low level of p-cofilin in the MB lobes had been previously shown

(Abe et al., 2014). In contrast to LIMK1, p-cofilin level was low in Cal formed by PN and KC terminals and high in cell nuclei. The latter corresponds to its functioning in the cell, as cofilin phosphorylation is necessary for its translocation into the nucleus (Abe et al., 1993).

The effectiveness of *limk1* suppression at the RNA level was confirmed using Act-GAL4 activator in the whole *Drosophila* body. GAL4 was also active in specific brain areas of the corresponding strains. However, we failed to quantitatively check the changes of *limk1* expression in *Drosophila* UAS × GAL4 hybrids with neuronal-specific GAL4 expression. The decrease in LIMK1 level might be local or too small. *limk1* interference might also induce the compensatory activation of LIMK1 translation.

To study *limk1* knockdown effects on memory, we used CCSP modification applied by (Kamyshev et al., 1999): training was performed with the mated female. In this case, courtship learning results from the rise of sensitivity to the antiaphrodisiac cis-vaccenyl acetate (cVA) due to unsuccessful courtship. cVA is not required for learning, being necessary for memory performance. aSP13 DAN, which innervate the *fru*-positive tip of γL, are necessary and sufficient for courtship learning (Keleman et al., 2012). 24 h memory consolidation requires the prolonged aSP13 stimulation and Orb2 dimerization in some γ neurons (Krüttner et al., 2015). α/β neurons are involved in LTM processes (Redt-Clouet et al., 2012; Jones et al., 2018). Hence, other DAN innervating α/βL of MB, including PAM and PPL1 cells (Aso et al., 2014a), may also be involved in LTM.

The behavioral differences were observed after *limk1* interference, e. g., the restoration of 3 h STM for *limk1-KD* > 6794 strain. GAL4 drivers themselves affected memory abilities, which were generally decreased compared to *CS*. The drivers also significantly affected the forgetting curves. Thus, we studied the effects of *limk1* interference relative to a control strain with the same GAL4 driver. We applied two different crossing schemes – UAS (f) > 6794 (m) (for 3 h STM and LTM analysis) and reverse (in the other behavioral experiments). In the first case, the control UAS > *limk1*"+" hybrid had bright eyes due to *v[1]* recessive allele, in contrast to UAS > *limk1-KD* hybrid with the wild type dark red eyes. The observed 3 h STM differences are unlikely to be associated with the differences in eyes pigmentation, as *v[1]* flies showed a normal 3 h STM and 2 day LTM in CCSP (Nikitina et al., 2021), while both forms of memory were impaired in the control strain. However, memory retention depends on parent affect, with some paternal epigenetic factors affecting STM strength (Medvedeva et al., 2021). For 6794 > *limk1-KD* strain, we did not see STM difference from the control strain, though learning ability slightly increased after *limk1* knockdown (see Fig. 5). Thus, when studying LIMK1 effects on learning and memory, it is necessary to consider the crossing direction.

Acetylcholine is the major excitatory neurotransmitter in *Drosophila*. Among CNH are: PN forming synapses on KC of MB (Yasuyama et al., 2002), the MB intrinsic neurons that are responsible for olfactory memory, expressing ChAT and VAChT (Barnstedt et al., 2016), and the α/β core neurons required for LTM consolidation (Yi et al., 2013). In the hybrids with 6793 driver (GAL4 expressed in CHN), GFP level was specifically high in α/βL compared to the other MB lobes. Here, *limk1* interference resulted in faster STM forgetting. This contradicts the cofilin role in active forgetting shown in OAVL, where cofilin was proposed to be regulated by LIMK1 (Shuai, Zhong, 2010). The involvement of LIMK1 and cofilin in forgetting may occur locally, within specific neuronal populations or synaptic terminals. At the same time, LIMK1 may be crucial for memory storage and retrieval in CCSP. The glutamatergic MBON M6 neurons serve for STM output: aSP13 DAN prolongs potentiation of γL – M6 synapses (Zhao et al., 2018). Some cholinergic MBON appeared to regulate the *Drosophila* visual appetitive memory (Aso et al., 2014b). As the extrinsic MB cells responsible for CCSP memory were similar to those used for appetitive memory (Montague, Baker, 2016), the decrease in 60 min STM might occur due to *limk1* suppression in some of these neurons.

The hybrids with 7009 driver (DAN and SRN) showed generally low CI values and negative LI values 24 h after learning. Males of these strains had pale pink eyes because of defects of eyes pigmentation, due to non-complete *w[1118]* rescue. *w[1118]* males demonstrated low courtship activity and success, presumably due to some defects of sexual development and maturation (Xiao et al., 2017). However, the control 7009 > *limk1*"+" strain had normal LI up to 60 min after training. *limk1* knockdown by 7009 driver was associated with dramatic defects of learning and memory: LI just after training did not statistically differ from zero. Thus, LIMK1-dependent signaling in DAN and SRN seems to be important for learning and memory in CCSP.

limk1 knockdown by 30027 driver (FRN) decreased the forgetting rate in the time interval 30–60 min. This corresponds to the role of actin-remodeling pathway in forgetting in OAVL paradigm (Shuai et al., 2010). LI of the control strain did not differ from zero starting from 30 min after learning, while *limk1* knockdown increased it. In males, FRN are responsible for courtship behavior. There are ~1500 FRN in the *Drosophila* brain, including sensory organs, lateral horn, lateral protocerebrum, SMP arch and motor control centers. Together they provide multisensory integration to regulate the male courtship process (Yu et al., 2010; Liu et al., 2019). Some CHN and DAN are also Fru-positive, such as ~300 γL neurons and aSP13 DAN located in SMP, which regulates courtship learning and memory. The activity of *fru* gene was reported to decrease upon LTM formation in CCSP (Winbush et al., 2012). Hence, suppression of some FRN activity may be associated with memory prolongation and consolidation.

In addition to memory processes, *limk1* interference affected some parameters of the male courtship song. As well as for courtship memory, we observed the opposite functional effects of *limk1* knockdown in FRN and CHN. FRN of the P1 class initiate *Drosophila* courtship behavior and trigger courtship song. pIP10 neurons possibly convey the P1 signal to thoracic dPR1 and vPR6 neurons, proposed to be the parts of a central pattern generator (CPG), which defines the time and shape of the pulse song. vPR6 possibly encode IPI (von Philipsborn et al., 2011). Pulse and sine CPG either contain FRN or interact with them. As sine and pulse song normally do not overlap, the mutually inhibitory mechanisms must exist, switching

between quasilinear and relaxation modes of oscillation for sine and pulse song, respectively. Some descending interneurons may control the type of the song, while the others trigger singing or terminate the song (Clyne, Miesenböck, 2008).

Indeed, we observed the opposite changes of PInd/PFr and SInd/SDur upon *limk1* interference in CHN and FRN, moving the balance toward the sine and pulse song, respectively. The increase in PFr after *limk1* knockdown in FRN might indicate the negative role of LIMK1-dependent signaling on activity of the pulse CPG or the upstream brain centers, which switch them from active to silent mode. CC is important for control of stability of pacemakers, which regulate the rhythmic structure of courtship song. PB destruction leads to sound signal distortions, FB and EB destruction additionally decreases sine and pulse trains (Popov et al., 2004). CC includes a large number of neuronal types, such as CHN, DAN, SRN, and others. CHN are present in FB, EB, No and PB (Kahsai, Winther, 2011), similarly to what we observed in our research. Hence, they probably play some role in regulation of male singing. The opposite effects of *limk1* interference in CHN and FRN may indicate a specific role of LIMK1 in courtship controlling network, whereas the other parts of the brain possibly have a total antagonistic effects on its activity. Alternatively, CHN and FRN *fru* neurons may differ in some aspects of regulation of LIMK1-dependent signaling pathway.

Conclusion

In summary, we have shown that effects of *limk1* interference in *Drosophila* male courtship memory and song depend on both the neuronal type and specific behavioral parameter. *limk1* interference in CHN and FRN had generally opposite effects, whereas its suppression in DAN and SRN impaired the flies' ability to learn. Using activator strains with a narrower pattern of GAL4 expression would help to better localize the brain structures, where LIMK1 regulates memory and forgetting in CCSP. Among such putative structures are γL and aSP13 DAN innervating γ5 area, as well as other DAN participating in memory formation, consolidation and retrieval. Studying the behavioral consequences of *limk1* overexpression in different brain areas will complement the estimates of the effects of its suppression. The above investigation should also focus on LIMK1 partner proteins, such as cofilin in its active and phosphorylated form.

References

Abe H., Nagaoka R., Obinata T. Cytoplasmic localization and nuclear transport of cofilin in cultured myotubes. *Exp. Cell Res.* 1993; 206(1):1-10. DOI 10.1006/excr.1993.1113.

Abe T., Yamazaki D., Murakami S., Hiroi M., Nitta Y., Maeyama Y., Tabata T. The NAV2 homolog Sickie regulates F-actin-mediated axonal growth in *Drosophila* mushroom body neurons *via* the non-canonical Rac-Cofilin pathway. *Development.* 2014;141(24):4716-4728. DOI 10.1242/dev.113308.

Albin S.D., Kaun K.R., Knapp J.M., Chung P., Heberlein U., Simpson J.H. A subset of serotonergic neurons evokes hunger in adult *Drosophila*. *Curr. Biol.* 2015;25(18):2435-2440. DOI 10.1016/j.cub.2015.08.005.

Aso Y., Grübel K., Busch S., Friedrich A.B., Siwanowicz I., Tanimoto H. The mushroom body of adult *Drosophila* characterized by GAL4 drivers. *J. Neurogenet.* 2009;23(1-2):156-172. DOI 10.1080/01677060802471718.

Aso Y., Hattori D., Yu Y., Johnston R.M., Iyer N.A., Ngo T.B., Dionne H., Abbott L.F., Axel R., Tanimoto H., Rubin G.M. The neuronal architecture of the mushroom body provides a logic for associative learning. *eLife.* 2014a;3:e04577. DOI 10.7554/eLife.04577.

Aso Y., Sitaraman D., Ichinose T., Kaun K.R., Vogt K., Belliart-Guérin G., Plaçais P., Robie A.A., Yamagata N., Schnaitmann C., Rowell W.J., Johnston R.M., Ngo T.B., Chen N., Korff W., Nitabach M.N., Heberlein U., Preat T., Branson K.M., Tanimoto H., Rubin G.M. Mushroom body output neurons encode valence and guide memory-based action selection in *Drosophila*. *eLife.* 2014b; 3:e04580. DOI 10.7554/eLife.04580.

Barnstedt O., Owald D., Felsenberg J., Brain R., Moszynski J.P., Talbot C.B., Perrat P.N., Waddell S. Memory-relevant mushroom body output synapses are cholinergic. *Neuron.* 2016;89(6):1237-1247. DOI 10.1016/j.neuron.2016.02.015.

Ben Zablah Y., Zhang H., Gugustea R., Jia Z. LIM-kinases in synaptic plasticity, memory, and brain diseases. *Cells*. 2021;10(8):2079-2103. DOI 10.3390/cells10082079.

Berry J.A., Cervantes-Sandoval I., Nicholas E.P., Davis R.L. Dopamine is required for learning and forgetting in *Drosophila*. *Neuron.* 2012;74(3):530-542. DOI 10.1016/j.neuron.2012.04.007.

Berry J.A., Phan A., Davis R.L. Dopamine neurons mediate learning and forgetting through bidirectional modulation of a memory trace. *Cell Rep*. 2018;25(3):651-662. DOI 10.1016/j.celrep.2018.09.051.

Cervantes-Sandoval I., Chakraborty M., MacMullen C., Davis R.L. Scribble scaffolds a signalosome for active forgetting. *Neuron.* 2016;90(6):1230-1242. DOI 10.1016/j.neuron.2016.05.010.

Clyne J.D., Miesenböck G. Sex-specific control and tuning of the pattern generator for courtship song in *Drosophila*. *Cell.* 2008;133(2): 354-363. DOI 10.1016/j.cell.2008.01.050.

Cook K.R., Parks A.L., Jacobus L.M., Kaufman T.C., Matthews K.A. New research resources at the Bloomington *Drosophila* Stock Center. *Fly* (*Austin*). 2010;4(1):88-91. DOI 10.4161/fly.4.1.11230.

Cuberos H., Vallée B., Vourc'h P., Tastet J., Andres C.R., Bénédetti H. Roles of LIM kinases in central nervous system function and dysfunction. *FEBS Lett.* 2015;589(24 Pt.B):3795-3806. DOI 10.1016/j.febslet.2015.10.032.

Davis R.L., Zhong Y. The biology of forgetting – a perspective. *Neuron.* 2017;95(3):490-503. DOI 10.1016/j.neuron.2017.05.039.

Duffy J.B. GAL4 system in *Drosophila*: a fly geneticist's Swiss army knife. *Genesis.* 2002;34(1-2):1-15. DOI 10.1002/gene.10150.

Gao Y., Shuai Y., Zhang X., Peng Y., Wang L., He J., Zhong Y., Li Q. Genetic dissection of active forgetting in labile and consolidated memories in *Drosophila*. *Proc. Natl. Acad. Sci. USA*. 2019;116(42): 21191-21197. DOI 10.1073/pnas.1903763116.

Hartenstein V. Morphological diversity and development of glia in *Drosophila*. *Glia.* 2011;59(9):1237-1252. DOI 10.1002/glia.21162.

Iliadi K.G., Kamyshev N.G., Popov A.V., Iliadi N.N., Rashkovetskaya E.L., Nevo E., Korol A.B. Peculiarities of the courtship song in the *Drosophila melanogaster* populations adapted to gradient of microecological conditions. *J. Evol. Biochem. Physiol.* 2009;45(5): 579-588. DOI 10.1134/S0022093009050041.

Jones S.G., Nixon K.C.J., Chubak M.C., Kramer J.M. Mushroom body specific transcriptome analysis reveals dynamic regulation of learning and memory genes after acquisition of long-term courtship memory in *Drosophila*. *G3: Genes Genomes Genetics* (*Bethesda*). 2018;8(11):3433-3446. DOI 10.1534/g3.118.200560.

Kahsai L., Winther A.M. Chemical neuroanatomy of the *Drosophila* central complex: distribution of multiple neuropeptides in relation to neurotransmitters. *J. Comp. Neurol.* 2011;519(2):290-315. DOI 10.1002/cne.22520.

Kamyshev N.G., Iliadi K.G., Bragina J.V. *Drosophila* conditioned courtship: two ways of testing memory. *Learn. Mem*. 1999;6(1): 1-20.

Kasture A.S., Hummel T., Sucic S., Freissmuth M. Big lessons from tiny flies: *Drosophila melanogaster* as a model to explore dysfunction of dopaminergic and serotonergic neurotransmitter systems. *Int. J. Mol. Sci.* 2018;19(6):1788-1805. DOI 10.3390/ijms19061788.

Keleman K., Vrontou E., Krüttner S., Yu J.Y., Kurtovic-Kozaric A., Dickson B.J. Dopamine neurons modulate pheromone responses in *Drosophila* courtship learning. *Nature.* 2012;489(7414):145-149. DOI 10.1038/nature11345.

Krüttner S., Traunmüller L., Dag U., Jandrasits K., Stepien B., Iyer N., Fradkin L.G., Noordermeer J.N., Mensh B.D., Keleman K. Synaptic Orb2A bridges memory acquisition and late memory consolidation in *Drosophila*. *Cell Rep.* 2015;11(12):1953-1965. DOI 10.1016/j.celrep.2015.05.037.

Liu W., Ganguly A., Huang J., Wang Y., Ni J.D., Gurav A.S., Aguilar M.A., Montell C. Neuropeptide F regulates court-ship in *Drosophila* through a male-specific neuronal circuit. *eLife.* 2019;8:1-29. DOI 10.7554/eLife.49574.

Lopatina N.G., Zachepilo T.G., Chesnokova E.G., Savateeva-Popova E.V. Mutations in structural genes of tryptophan metabolic enzymes of the kynurenine pathway modulate some units of the L-glutamate receptor – actin cytoskeleton signaling cascade. *Russ. J. Genet.* 2007;43(10):1168-1172. DOI 10.1134/S1022795407100110.

Mao Z., Davis R.L. Eight different types of dopaminergic neurons innervate the *Drosophila* mushroom body neuropil: anatomical and physiological heterogeneity. *Front. Neural Circuits.* 2009;3:1-17. DOI 10.3389/neuro.04.005.2009.

Mazzoni D., Dannenberg R. Audacity®. Audacity Team, 2020. URL: https://audacityteam.org. Last access: 05.12.2021.

Medina J.H. Neural, cellular and molecular mechanisms of active forgetting. *Front. Syst. Neurosci.* 2018;12:1-10. DOI 10.3389/fnsys.2018.00003.

Medvedeva A.V., Molotkov D.A., Nikitina E.A., Popov A.V., Karagodin D.A., Baricheva E.M., Savvateeva-Popova E.V. Systemic regulation of genetic and cytogenetic processes by a signal cascade of actin remodeling: locus *agnostic* in *Drosophila*. *Russ. J. Genet.* 2008;44(6):669-681. DOI 10.1134/S1022795408060069.

Medvedeva A.V., Tokmatcheva E.V., Kaminskaya A.N., Vasileva S.A., Nikitina E.A., Zhuravlev A.V., Zakharov G.A., Zatsepina O.G., Savvateeva-Popova E.V. Parent-of-origin effects on nuclear chromatin organization and behavior in a *Drosophila* model for Williams–Beuren Syndrome. *Vavilovskii Zhurnal Genetiki i Selektsii = Vavilov Journal of Genetics and Breeding*. 2021;25(5):472-485. DOI 10.18699/VJ21.054.

Montague S.A., Baker B.S. Memory elicited by courtship conditioning requires mushroom body neuronal subsets similar to those utilized in appetitive memory. *PLoS One.* 2016;11(10):e0164516. DOI 10.1371/journal.pone.0164516.

Ng J., Luo L. Rho GTPases regulate axon growth through convergent and divergent signaling pathways. *Neuron.* 2004;44(5):779-793. DOI 10.1016/j.neuron.2004.11.014.

Nikitina E.A., Medvedeva A.V., Zakharov G.A., Savvateeva-Popova E.V. The *Drosophila* agnostic locus: involvement in the formation of cognitive defects in Williams syndrome. *Acta Naturae.* 2014;6(2):53-61. DOI 10.32607/20758251-2014-6-2-53-61.

Nikitina E.A., Zhuravlev A.V., Savvateeva-Popova E.V. Effect of impaired kynurenine synthesis on memory in *Drosophila*. *Integrativnyaya Fiziologiya = Integrative Physiology*. 2021;2(1):49-60. DOI 10.33910/2687-1270-2021-2-1-49-60. (in Russian)

Okamoto N., Nishimura T. Signaling from glia and cholinergic neurons controls nutrient-dependent production of an insulin-like peptide for *Drosophila* body growth. *Dev. Cell.* 2015;35(3):295-310. DOI 10.1016/j.devcel.2015.10.003.

Popov A.V., Peresleni A.I., Savvateeva-Popova E.V., Vol'f R., Heisenberg M. The role of the mushroom bodies and of the central complex of *Drosophila melanogaster* brain in the organization of courtship behavior and communicative sound production. *J. Evol. Biochem. Phys.* 2004;40:641-652. DOI 10.1007/s10893-004-0005-z.

Redt-Clouet C., Trannoy S., Boulanger A., Tokmatcheva E., Savvateeva-Popova E., Parmentier M.L., Preat T., Dura J.M. Mushroom body neuronal remodelling is necessary for short-term but not for long-term courtship memory in *Drosophila*. *Eur. J. Neurosci.* 2012;35(11):1684-1691. DOI 10.1111/j.1460-9568.2012.08103.x.

Ritchie M.G., Yate V.H., Kyriacou C.P. Genetic variability of the interpulse interval of courtship song among some European populations of *Drosophila melanogaster*. *Heredity* (*Edinb*). 1994;72(Pt.5):459-464. DOI 10.1038/hdy.1994.64.

Salvaterra P.M., Kitamoto T. *Drosophila* cholinergic neurons and processes visualized with Gal4/UAS-GFP. *Brain Res. Gene Expr. Patterns.* 2001;1(1):73-82. DOI 10.1016/s1567-133x(01)00011-4.

Savvateeva-Popova E.V., Popov A.V., Grossman A., Nikitina E.A., Medvedeva A.V., Peresleni A.I., Molotkov D.A., Kamyshev N.G., Pyatkov K.I., Zatsepina O.G., Schostak N., Zelentsova E.S., Pavlova G., Panteleev D., Riederer P., Evgen'ev M.B. Non-coding RNA as a trigger of neuropathologic disorder phenotypes in transgenic *Drosophila*. *J. Neural Transm.* (*Vienna*). 2008;115(12):1629-1642. DOI 10.1007/s00702-008-0078-8.

Savvateeva-Popova E.V., Popov A.V., Heinemann T., Riederer P. *Drosophila* mutants of the kynurenine pathway as a model for ageing studies. *Adv. Exp. Med. Biol.* 2003;527:713-722. DOI 10.1007/978-1-4615-0135-0_84.

Savvateeva-Popova E.V., Zhuravlev A.V., Brázda V., Zakharov G.A., Kaminskaya A.N., Medvedeva A.V., Nikitina E.A., Tokmatcheva E.V., Dolgaya J.F., Kulikova D.A., Zatsepina O.G., Funikov S.Y., Ryazansky S.S., Evgen'ev M.B. *Drosophila* model for the analysis of genesis of LIM-kinase 1-dependent Williams–Beuren syndrome cognitive phenotypes: INDELs, transposable elements of the Tc1/*mariner* superfamily and microRNAs. *Front. Genet*. 2017;8:123. DOI 10.3389/fgene.2017.00123.

Shuai Y., Lu B., Hu Y., Wang L., Sun K., Zhong Y. Forgetting is regulated through Rac activity in *Drosophila*. *Cell.* 2010;140(4):579-589. DOI 10.1016/j.cell.2009.12.044.

Shuai Y., Zhong Y. Forgetting and small G protein Rac. *Protein Cell.* 2010;1(6):503-506. DOI 10.1007/s13238-010-0077-z.

Siegel R.W., Hall J.C. Conditioned responses in courtship behavior of normal and mutant *Drosophila*. *Proc. Natl. Acad. Sci. USA.* 1979;76(7):3430-3434. DOI 10.1073/pnas.76.7.343.

Strauss R., Heisenberg M. A higher control center of locomotor behavior in the *Drosophila* brain. *J. Neurosci.* 1993;13(5):1852-1861. DOI 10.1523/JNEUROSCI.13-05-01852.1993.

Sun B., Xu P., Salvaterra P.M. Dynamic visualization of nervous system in live *Drosophila*. *Proc. Natl. Acad. Sci. USA.* 1999;96(18):10438-10443. DOI 10.1073/pnas.96.18.10438.

Thapa A., Sullivan S.M., Nguyen M.Q., Buckley D., Ngo V.T., Dada A.O., Blankinship E., Cloud V., Mohan R.D. Brief freezing steps lead to robust immunofluorescence in the *Drosophila* nervous system. *Biotechniques.* 2019;67(6):299-305. DOI 10.2144/btn-2018-0067.

Tully T., Preat T., Boynton S.C., Vecchio M.D. Genetic dissection of consolidated memory in *Drosophila*. *Cell.* 1994;79(1):35-47. DOI 10.1016/0092-8674(94)90398-0.

Virtual Fly Brain. URL: https://v2.virtualflybrain.org. Last access: 01.12.2021.

von Philipsborn A.C., Liu T., Yu J.Y., Masser C., Bidaye S.S., Dickson B.J. Neuronal control of *Drosophila* courtship song. *Neuron.* 2011;69(3):509-522. DOI 10.1016/j.neuron.2011.01.011.

Winbush A., Reed D., Chang P.L., Nuzhdin S.V., Lyons L.C., Arbeitman M.N. Identification of gene expression changes associated with long-term memory of courtship rejection in *Drosophila* males. *G3: Genes Genomes Genetics* (*Bethesda*). 2012;2(11):1437-1445. DOI 10.1534/g3.112.004119.

Xiao C., Qiu S., Robertson R.M. The white gene controls copulation success in *Drosophila melanogaster*. *Sci. Rep.* 2017;7(1):7712-7725. DOI 10.1038/s41598-017-08155-y.

Yasuyama K., Meinertzhagen I.A., Schürmann F.W. Synaptic organization of the mushroom body calyx in *Drosophila melanogaster*. *J. Comp. Neurol.* 2002;445(3):211-226. DOI 10.1002/cne.10155.

Yi W., Zhang Y., Tian Y., Guo J., Li Y., Guo A. A subset of cholinergic mushroom body neurons requires Go signaling to regulate sleep in *Drosophila*. *Sleep.* 2013;36:1809-1821. DOI 10.5665/sleep.3206.

Yu J.Y., Kanai M.I., Demir E., Jefferis G.S., Dickson B.J. Cellular organization of the neural circuit that drives *Drosophila* courtship behavior. *Curr. Biol.* 2010;20(18):1602-1614. DOI 10.1016/j.cub.2010.08.025.

Zalomaeva E.S., Falina V.S., Medvedeva A.V., Nikitina E.A., Savvateeva-Popova E.V. Learning and forgetting in *Drosophila melanogaster* in *limk1* gene polymorphism. *Integrativnyaya Fiziologiya* = *Integrative Physiology.* 2021;2(3):318-327. DOI 10.33910/2687-1270-2021-2-3-318-327. (in Russian)

Zhang X., Li Q., Wang L., Liu Z.J., Zhong Y. Cdc42-dependent forgetting regulates repetition effect in prolonging memory retention. *Cell Rep*. 2016;16(3):817-825. DOI 10.1016/j.celrep.2016.06.041.

Zhao X., Lenek D., Dag U., Dickson B.J., Keleman K. Persistent activity in a recurrent circuit underlies courtship memory in *Drosophila*. *eLife.* 2018;7:1-16. DOI 10.7554/eLife.31425.

Zhuravlev A.V., Shchegolev B.F., Zakharov G.A., Ivanova P.N., Nikitina E.A., Savvateeva-Popova E.V. 3-Hydroxykynurenine as a potential ligand for Hsp70 proteins and its effects on *Drosophila* memory after heat shock. *Mol. Neurobiol.* 2022;59(3):1862-1871. DOI 10.1007/s12035-021-02704-3.

Zhuravlev A.V., Vetrovoy O.V., Ivanova P.N., Savvateeva-Popova E.V. 3-Hydroxykynurenine in regulation of *Drosophila* behavior: the novel mechanisms for cardinal phenotype manifestations. *Front. Physiol.* 2020;11:971. DOI 10.3389/fphys.2020.00971.

ORCID ID

A.V. Zhuravlev orcid.org/0000-0003-2673-4283
E.S. Zalomayeva orcid.org/0000-0002-6005-3433
E.S. Egozova orcid.org/0000-0002-0055-3778
A.D. Emelin orcid.org/0000-0002-8498-9017
V. V. Sokurova orcid.org/0000-0003-0821-9974
E.A. Nikitina orcid.org/0000-0003-1897-8392
E.V. Savvateeva-Popova orcid.org/0000-0002-6925-4370

Acknowledgements. This research was funded by the Russian Foundation for Basic Research (No. 20-015-00300 A). We thank Prof. E. Buchner (Institute of Clinical Neurobiology, Würzburg) for Drosophila anti-CSP antibodies. We also thank the Bloomington Drosophila Stock Center (NIH P40OD018537) at Indiana University (USA) and TRiP at Harvard Medical School (NIH/NIGMS R01-GM084947) for providing us with transgenic GAL4 and UAS fly stocks. This study was supported by the State Program 47 GP "Scientific and Technological Development of the Russian Federation" (2019–2030), theme 0134-2019-0004.

Conflict of interest. The authors declare no conflict of interest.

Received June 9, 2022. Revised August 19, 2022. Accepted August 24, 2022.